



Deletion of Interleukin 1 Receptor-Associated Kinase 1 Improves TLR4/STAT1/PPAR γ -Cd36 Signaling-Mediated Alcoholic Fatty Liver



Shujing Li^{1,2}, Xiaojian Sun³, Hongxia Chen¹, Jingqing Liang¹, Minjie Chen¹, Su Xu¹, Xicui Sun¹, Liya Pi⁴, Bin Ren⁵, Zhegang Ying⁶, Li Zhang⁷, Qi Cao^{1*}

¹Department of Diagnostic Radiology and Nuclear Medicine, University of Maryland School of Medicine, USA

²Department of Radiology, The first affiliated Hospital of Hebei Medical University, P.R. China

³Department of Endocrinology, Diabetes and Nutrition, Department of Medicine, University of Maryland School of Medicine, USA

⁴Department of Pediatrics in the College of Medicine, University of Florida, USA

⁵Department of Surgery, University of Alabama at Birmingham School of Medicine, USA

⁶Department of Medicine, University of Maryland School of Medicine, USA

^{7,8}The School of Basic Medical Sciences, Wuhan University, P.R. China

Submission: December 01, 2021; **Published:** December 14, 2021

*Corresponding author: Qi Cao, Department of Diagnostic Radiology and Nuclear Medicine, University of Maryland School of Medicine, Baltimore, Maryland, USA

Abstract

Background and Aims: IRAK1 axis has been impacted in ethanol-induced liver disease as a signal transduction pathway and influencing gene transcription in hepatic cells. As an established technique, proton magnetic resonance spectroscopy (1H-MRS) can semi quantify relative hepatic lipid levels as percentage of total liver water in fatty liver disease. We aimed to investigate the accuracy of quantitative liver lipids by converting 1H-MRS measurements of semiquantitative liver lipids with reliable and repeatable ex vivo measurement of absolute amount of liver water in alcoholic-induced fatty liver disease model in mice using the liquid ethanol diet-fed and to characterize the lipid mechanism and the molecular mediators which are related to lipid metabolism in liver under ethanol exposure or combined with IRAK1 knock-out in mice.

Methods: Twenty-four C57BL/6 mice were assigned into four groups (alcoholic liver fatty (AFL), control (Ctr), wide type (WT) and knock-out (KO) groups). Twelve weeks after feeding, in vivo 1H MRS measurement of semiquantitative hepatic lipids was performed and the results were used to calculate absolute amount of liver lipids and these data were compared with liver triglyceride (TG) and cholesterol measured by biochemistry assays. RTPCR analysis and western blotting analysis were performed to measure the expression of TLR4/2, IRAK1, STAT1, PPAR α , PPAR γ , CD36, FOXO1 and p-FOXO1.

Results: Absolute amount of liver lipids was higher in AFL and WT model mice than that of Ctr (0.32 \pm 0.07 versus 0.03 \pm 0.005, p<0.001). IRAK1 gene knockdown showed ethanol-induced steatosis was completely abolished. There were strong correlations of absolute liver lipid concentrations to their liver TG, cholesterol and TG + cholesterol measured by biochemical assays in the four groups. Ethanol diet significantly up-regulates the phosphorylation of TLR4, IRAK1, STAT1, PPAR α , PPAR γ , CD36, and FOXO1 in ALF and WT mice, while down-regulating p-FOXO1 expression compared to Ctr. However, these changes were reversed in IRAK1 -/- mice.

Conclusion: IRAK1 knock out has a great protective effect on ethanol-induced hepatic injury. Our study clarified that IRAK1 knock out can inhibit fat synthesis in alcoholic fatty liver disease through TLR-IRAK1-PPAR-CD36-FOXO1 pathway and CD36 plays critical role in the pathway.

Keywords: Alcoholic fatty liver disease; Proton magnetic resonance spectroscopy; Hepatic steatosis; interleukin-1 receptor-associated kinase 1; CD36; Triglyceride; Cholesterol

Abbreviations: AFLD: Alcoholic Fatty Liver Disease; TLR: Toll-Like Receptor; IRAK1: Interleukin-1 Receptor Associated Kinase 1; STAT1: Signal Transducer and Activator of Transcription1; PPAR α : Peroxisome Proliferator-Activated Receptor Alpha; PPAR γ : Peroxisome Proliferator-Activated Receptor Gamma; FOXO1: Fork Head Box Protein 01; p- FOXO1: Phospho-FOXO1; ALT: Alanine Aminotransferase; AST: Aspartate Aminotransferase; RT-PCR: Real-Time Polymerase Chain Reaction

Introduction

Alcoholic fatty liver disease (AFLD) is one of the earliest forms of liver injury and approximately 20% of patients with simple steatosis may develop into more severe forms of liver

injury, including steatohepatitis, fibrosis, cirrhosis, and eventually hepatocellular carcinoma [1] if action of appropriate management is not taken. It has not been established that non-invasive techniques quantifies absolute amount of liver lipids in an early

and mild steatosis because imaging modalities have limitation of sensitivity and specificity. The association between chronic alcohol consumption and the development of alcoholic liver disease is a well-known phenomenon, but the precise underlying molecular mediators involved in ethanol-induced liver disease remain elusive. Toll-like receptor (TLR) -mediated inflammatory-signaling pathways are shown to be associated with AFLD [2] via complex immune responses mediating hepatocyte (i.e., hepatocellular injury and regeneration) or hepatic stellate cell (i.e., fibrosis and cirrhosis) inflammatory or immune pathologies in animal models [3,4] and human livers [5]. Interleukin-1 receptor-associated kinase 1 (IRAK1) are serine/threonine kinases that play critical roles in closely involving non-alcoholic fatty liver disease (NAFLD) [6] and immune responses through their role in TLR-mediated signaling pathways [7]. Several studies have shown that the signal transducer and activator of transcription1 (STAT1) played key role in regulation of liver metabolism [8,9]. Peroxisome proliferator-activated receptor alpha and gamma (PPAR α , PPAR γ) signal have been shown to regulate lipogenesis and lipid accumulation.

Several studies have shown that hepatic PPAR and PPAR is up-regulated in alcohol-induced liver injury by promoting hepatic steatosis and inflammation both in rats [10], mice [11] and human [12]. CD36 has been shown to play an important role in hepatic lipid homeostasis in animal [13] and human [14]. A study by Shirpoor and colleagues about the relationship between CD36 and ethanol-induced liver injury in rats has shown the hepatic abnormalities may in part be associated with lipid homeostasis changes mediated by overexpression of CD36 [15]. Long-term alcohol stimulation may inhibit the expression of silent information regulator 1 in hepatocytes, which increases the acetylation level of fork head box transcription factor O1 (FOXO1), reduces nuclear localization, and reduces the binding capacity of DNA sequence.

This further downregulates the expression of downstream adiponectin receptor 2 and microsomal triglyceride transfer protein, causes lipid metabolism disorders and triglyceride deposition in hepatocytes by affecting adiponectin signal transduction and synthesis of very-low-density lipoprotein, and finally promotes the development of alcoholic fatty liver disease [16]. In terms of the role of phospho-FOXO1(p-FOXO1) in lipid metabolism, a study by Zhu and colleagues has shown that the expression of p-FOXO1 in the liver tissues were up-regulated following supplementation with resveratrol which was able to attenuate hepatic steatosis and lipid metabolic disorder in mice model [17]. The aim of this study was to investigate the accuracy of quantitative liver lipids by converting ¹H-MRS measurements of semiquantitative liver lipids with reliable and repeatable ex vivo measurement of absolute amount of liver water in a mouse alcoholic-induced fatty liver model and to investigate the deletion of IRAK1 improves TLR4/STAT1/PPAR-CD36 signaling mediated alcoholic fatty liver quantified by ¹H MRS.

Materials and Methods

Animals and alcoholic fatty liver model

C57BL/6 mice (18–20 g, 6 weeks of age) were purchased from the Charles River Laboratories (Wilmington, Massachusetts). The mice were housed in a sterile plastic cage under controlled conditions (temperature, 20–22°C and humidity, 50±10%). The experiment was ethically approved by the Institutional Animal Care and Use Committee of University of Maryland School of medicine and performed in accordance with the National Institute of Health and University Guidelines for Laboratory Animals Care and Usage. The detailed animal feeding protocol and diet composition were described according to the modified method of Xu et al. [18]. The C57BL/6 mice were divided into 4 groups (n=6 per group): 1) alcohol fatty liver (AFL) with liquid ethanol diet-fed mice; 2) isocaloric controls (Ctr) mice; 3) liquid ethanol diet-fed wild type mice (WT); 4) liquid ethanol diet-fed insulin resistance-associated knockout1 (IRAK1) (-/-) mice (KO).

The mice were sacrificed 15 hours after the liver imaging at 12 weeks after feeding ethanol diet, and blood samples were immediately withdrawn from the left ventricle. Plasma triglyceride (TG, Bio vision, Milpitas, CA) and cholesterol (Chol, Bio vision, Milpitas, CA), alanine aminotransferase (ALT, Sigma-Aldrich, St Louis, MO), and aspartate aminotransferase (AST, Sigma-Aldrich, St Louis, MO) levels were determined according to the methods of Cao et al. [19]. Liver tissues were removed for measurement of liver water by baking spliced liver samples in a 60°C oven, and histological examination by H&E and Masson's trichrome staining, lipids by biochemistry assays.

7.0 T ¹H-MRS measurements of liver lipids and data analyses

¹H-MRS measurements of liver lipids were performed on a Bruker BioSpec 70/30USR Avance III 7 T horizontal bore MR scanner (Bruker Biospin MRI GmbH, Ettlingen, Germany). During the experiment, all mice were anesthetized with isoflurane/air at 1 to 2%/L/min oxygen) with compatible small-animal and respiratory monitoring. MR imaging were collected using Multislice proton-density-weighted and T2-weighted Rapid Acquisition with Relaxation Enhancement (RARE) sequence with TR=3000ms, TE1/TE2 = 9.2/27.6 ms, slice thickness=1mm, number of slices =12, field of view (FOV) = 3.5×3.5 cm², matrix size=128×128, number of excitation (NEX) = 2. The volume of interest (VOI) of the subsequent proton spectroscopy was carefully planned on homogeneous liver parenchyma to avoid contributions from obvious blood vessels, subcutaneous fat, and air. The single-voxel was performed using a fully relaxed point-resolved spectroscopy (PRESS) sequence without water suppression with the following parameters: voxel volume 4×6×4 mm³, TR = 10000 ms, TE = 16.5 ms, 64 signal averages. All MR spectra were processed with Bruker Topspin package.

Calculation of total liver water and lipids

About 500 milligrams (mg) of liver tissue from each animal liver were cut and placed in a 60°C oven for 3 days. Dry liver weight in grams was measured at the end of each day and the amount of water evaporation from the liver tissue was calculated by deduction of dry liver weights from wet liver tissue weight. Total liver water each animal was calculated by multiplying whole liver tissue weight each animal with the percentages of water in its spliced liver tissue. Total liver lipids (mmol/gram wet liver weight) were calculated based on amounts of evaporated water and the ratio of total lipids to water by MRS.

Quantitative RT-PCR analysis

RNA was purified using the RNeasy kit (Qiagen Sciences, Maryland, USA) and on-column DNA digestion. cDNA was transcribed with the Reverse Transcription System (Promega Corp., Madison, WI). Real-time quantitative polymerase chain reaction was performed using the iCycler (Bio-Rad Laboratories Inc., Hercules, CA). The primer sequences were: TLR2, 5'-CTAGCTAGCTAGATGCTACGAGCTCTT-3' (sense) and 5'-CGCTCGAGCGGCTAGGCCTTTATTGC-3' (anti-sense); TLR4, 5'-GCTTTCACCTCTGCCTTCCAC-3' (sense) and 5'-GGCGATACAATTCACCTG-3' (anti-sense); IRAK1, 5'-ATGGCCGGGGGGCCGGGCCCGGGG-3' (sense) and 5'-CAGCTCTGGAATTCATCACTTTCT-3' (anti-sense); STAT1, 5'-AAATTTGTTTTTTGTTGGATTTTT-3' (sense) and 5'-ACCAATTAAACACAACACTATTCCATA-3' (anti-sense); CD36, 5'-GATGACGTGGCAAAGAACAG-3' (sense) and 5'-CCTCGGGGTCCTGAGTTAT-3' (anti-sense); GAPDH, 5'-AACTTTGGCATTGTGGAAGG-3' (sense) and 5'-CCTGTTGCTGTAGCCGTAT-3' (anti-sense).

Western blotting analysis

For western blotting studies, protein extracts were obtained from the mouse livers using a commercial lysis buffer (Bio-Rad, Hercules, Ca) that contained a protease inhibitor cocktail (Roche, Indianapolis, IN). The protein concentrations were determined with the bio-rad protein assay kit (Bio-rad, Hercules, Ca). The western blotting analysis was performed with antibodies that were specific to TLR2, TLR4, IRAK1, STAT1, PPAR γ , PPAR α , FOXO1, p-FOXO1, CD36, GAPDH, and Histone3 (Abcam, Cambridge, MA). After the sodium dodecyl sulfatepolyacrylamide gel electrophoresis at 15% acrylamide concentrations, the proteins were transferred to the nitrocellulose membrane and then exposed to the primary antibody.

Secondary antibody binding was visualized using a Super Signal Western Dura kit (Pierce, Grosse Pointe, MI). Protein bands were firstly normalized with corresponding GAPDH or histone 3 and band density and controls in each experiment were considered as reference of 1.

Statistics

All the values are represented as the mean \pm Standard error of the mean (SEM). The analysis of the variance (ANOVA) was used to compare significant differences among the groups. All analyses described here were conducted using Excel software. $P < 0.05$ was considered statistically significant.

Results

IRAK1 gene knock-down significantly reversed liquid ethanol diet-induced hepatic steatosis in IRAK1 $-/-$ mice

As we expected, significant increase in formations of steatosis, liver inflammation, and ballooning (Figure 1A-D) and trend increase in accumulation of collagen (Figure 1E-H) were identified in AFL and WT mice and corresponding scores of these liver lesions were summarized in (Figure 1K-N). Interestingly IRAK1 gene knockdown dramatically reversed these lesions. Body weight gain was not different among the four groups of mice (Figure 1I), but the ratio of liver to body weight was greater in AFL and WT mice than that of Ctr or KO mice (Figure 1J). Damaged hepatocyte released enzymes ALT and AST levels were significantly elevated in AFL and WT mice when compared with these in Ctr or KO mice (Figure 1O & 1P).

Absolute amount of total liver lipids calculated from liver water by in vivo ^1H -MRS, and liver TG, cholesterol, and TG + cholesterol levels by biochemistry assays

Accurate lipid peak located at 1.3ppm and water peak located at 4.7ppm were acquired with relative consistent water peak levels in Figure 2A-D. With *ex vivo* measurement of liver water and wet liver weight, absolute amount of liver lipids was calculated from percentages of liver lipids to water using ^1H MRS. Absolute amount of liver lipids was higher in AFL and WT model mice than that of Ctr (0.32 ± 0.07 versus 0.03 ± 0.005 , $p < 0.001$) (Figure 2E). IRAK1 gene knockdown showed ethanol-induced steatosis was completely abolished. In addition, liver TG and cholesterol levels were higher in AFL and WT compared to that of Ctr mice. This elevation of liver lipids was prevented after knockdown of IRAK1 gene (Figure 2F & 2G).

To verify whether absolute liver lipids converted from ^1H MRS and *ex vivo* measurement of liver water and liver weight reflects liver lipids measured by biochemistry assays, correlation analysis was performed and showed strong correlation between total liver lipids by MRS and liver TG ($R^2 = 0.8976, 0.9124, 0.8981, \text{ and } 0.9969$, respectively, Figure 3A-D), cholesterol ($R^2 = 0.9199, 0.8985, 0.9344, \text{ and } 0.9025$, respectively, Figure 3E-H) and TG + cholesterol ($R^2 = 0.9044, 0.9212, 0.831, \text{ and } 0.9327$, respectively, Figure 3I-L) in AFL, Ctr, WT, and KO mice.

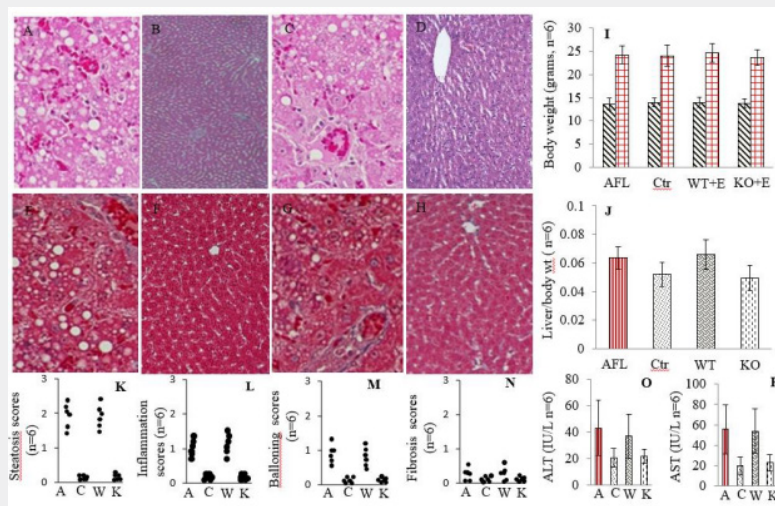


Figure 1: Decreased alcoholic steatosis in IRAK1 $-/-$ mice. (A-D) H&E staining for histopathological analysis. (E-H) Masson's trichrome staining for fibrosis. (I) Body weight change. (J) Ratio of liver to body weight. (K) Steatosis, (L) inflammation, (M) ballooning, and (N) fibrosis quantification. (O) ALT and (P) AST change. (AFL, alcoholic fatty liver; Ctr, control; WT, wild type; KO, IRAK1 knockout).

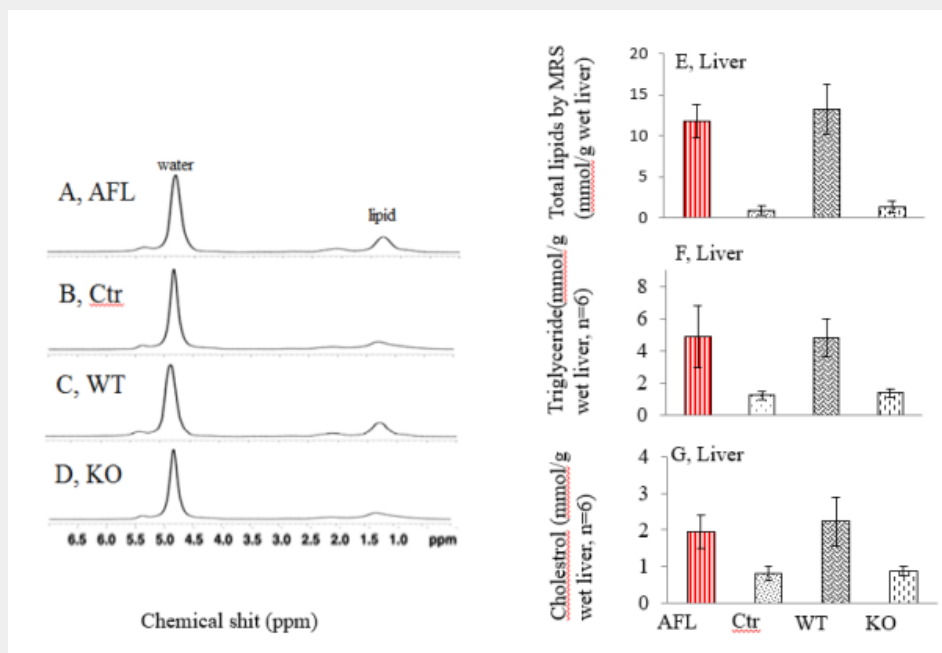


Figure 2: Liver lipids by MRS and kit assays. (A-D) Liver lipids and water in vivo 1H-MRS and corresponding voxel locations. (E) Total liver lipids, (F) liver triglyceride, and (G) liver cholesterol. (1H-MRS proton magnetic resonance spectroscopy; ppm, parts per million).

Decreased ethanol-induced expression of TLR4, but TLR2 in IRAK1 $-/-$ mice

Hepatic levels of TLR4 mRNA and protein significantly increased in AFL and WT mice compared with Ctr mice. IRAK1 KO mice slightly reversed levels of hepatic levels of TLR4 mRNA and protein compared with corresponding WT mice, but there is no significance between WT and KO mice (Figure 4A & 4B). However, no significant increase in hepatic levels of TLR2 mRNA and protein

was identified in AFL mice compared with Ctr mice and IRAK1 gene knockdown did not change TLR2 expression when compared with its corresponding WT mice (Figure 4C & 4D).

Completely blocked IRAK1 expression and significantly reversed STAT1 phosphorylation in IRAK1 $-/-$ mice

Given IRAK1 signal was reported as down-stream of TLRs, our PCR and western blot experiments showed elevated expression of IRAK1 was identified in AFL and WT mice, however, in our

IRAK1 $-/-$ mice liver tissues had absence of IRAK1 mRNA and protein expressions after ethanol feeding (Figure 5A & 5B). Given STAT1 protein was reported involvement in regulation of CD36 expression, our experiments showed significantly increased

phosphorylation of hepatic STAT1 in AFL and WT mice compared with Ctr mice. In IRAK1 $-/-$ mice the elevated level of STAT1 seen in AFL and WT mice was reduced to the level of Ctr mice (Figure 5C & 5D).

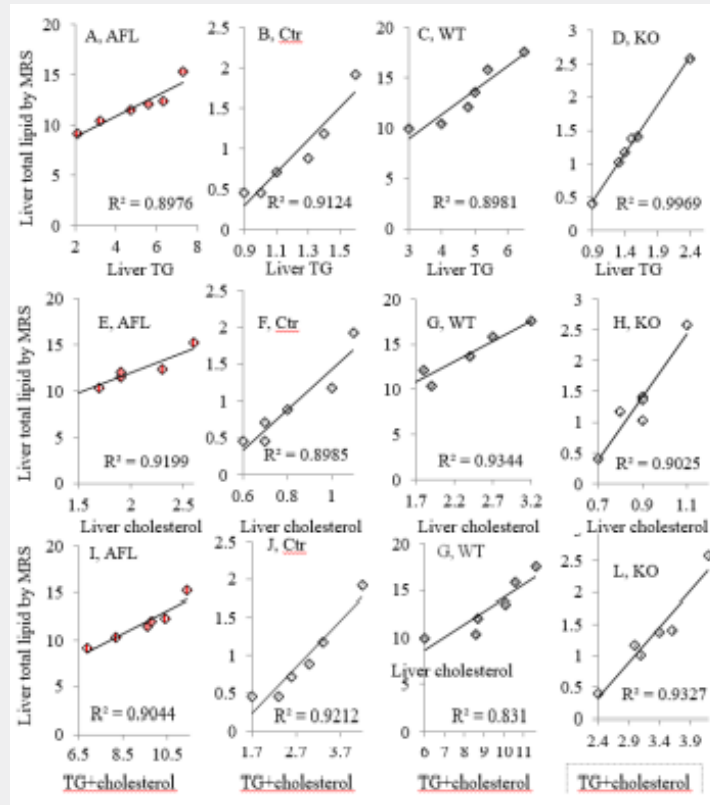


Figure 3: Correlation between liver lipids by MRS and kit assays. Correlation between total liver lipids by MRS and liver TG (A-D), cholesterol (E-H) and TG + Cholesterol (I-L). TG, triglyceride.

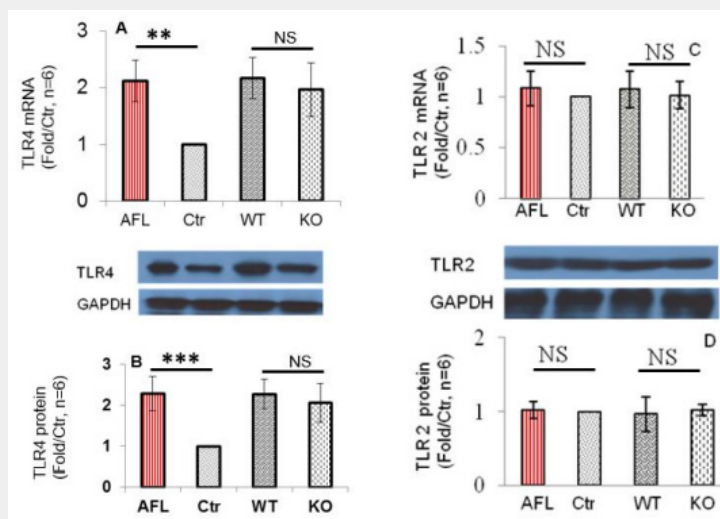


Figure 4: Decreased expressions of TLR4 gene and protein, but no changes of TLR2 expressions in IRAK1 $-/-$ mice. (A) Gene expressions of TLR 4 and (B) their protein in livers, (C) Gene expressions of TLR 2 and (D) their protein expressions in livers. NS: no significance, **: $P < 0.01$, and ***: $P < 0.001$ compared with controls.

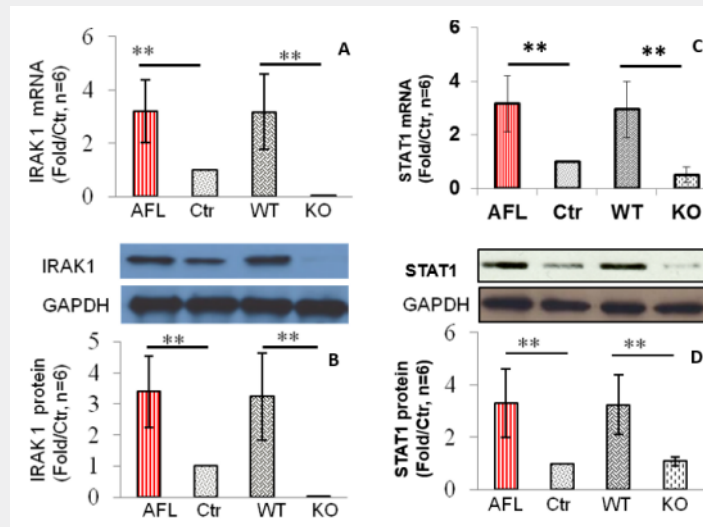


Figure 5: Almost no expressions of IRAK1 and decreased expressions of STAT1 gene and protein in IRAK1 ^{-/-} mice. (A) Gene expressions of IRAK1 and (B) their protein in livers, (C) Gene expressions of STAT1 and (D) their protein in livers. **: P<0.01 compared with controls.

Significantly reversed expression of PPAR, PPAR, and CD36 in IRAK1 ^{-/-} mice

Expression of PPAR α and PPAR γ was significantly induced in the liver of AFL and WT mice compared to Ctr mice, however, ethanol-induced expressions in WT mice livers were reversed in

IRAK1 KO mice (Figure 6A & 6B). The expression of CD36 mRNA and protein by RT-PCR and western blotting was significantly elevated in AFL and WT mice compared to Ctr mice and almost restored to similar levels in IRAK1 KO mice compared to the Ctr group (Figure 6C & 6D).

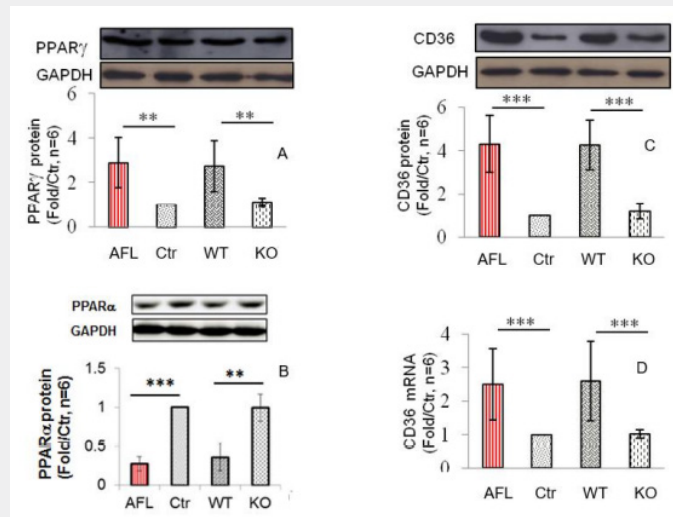


Figure 6: Decreased expressions of PPAR α , PPAR γ protein, CD36 gene and protein in IRAK1 ^{-/-} mice. (A) Expressions of PPAR α in livers, (B) Expressions of PPAR γ in livers. (C) Gene expressions of CD36 and (D) their protein in livers. **: P<0.01 and ***: P<0.001 compared with controls.

Decreased nuclear translocation of FOXO1 and increased nuclear translocation of pFOXO1 in IRAK1 ^{-/-} mice

Using western blotting experiments, we subsequently assessed the two fractional subcellular levels of FOXO1 and

p-FOXO1 in four groups. The expression of FOXO1 in both cytosol and nuclear significantly increased in ALF and WT mice compared to normal mice, but the levels of FOXO1 in nuclear were much higher than levels in cytosol. Phosphorylated FOXO1 levels were significantly reduced in nuclear and cytosol and relatively more

prominent decreased levels of phosphorylated FOXO1 were identified in nuclear. IRAK1 gene knockdown almost reversed

changes of FOXO1 and phosphorylated FOXO1 seen in ALF and WT mice (Figure 7A & 7B).

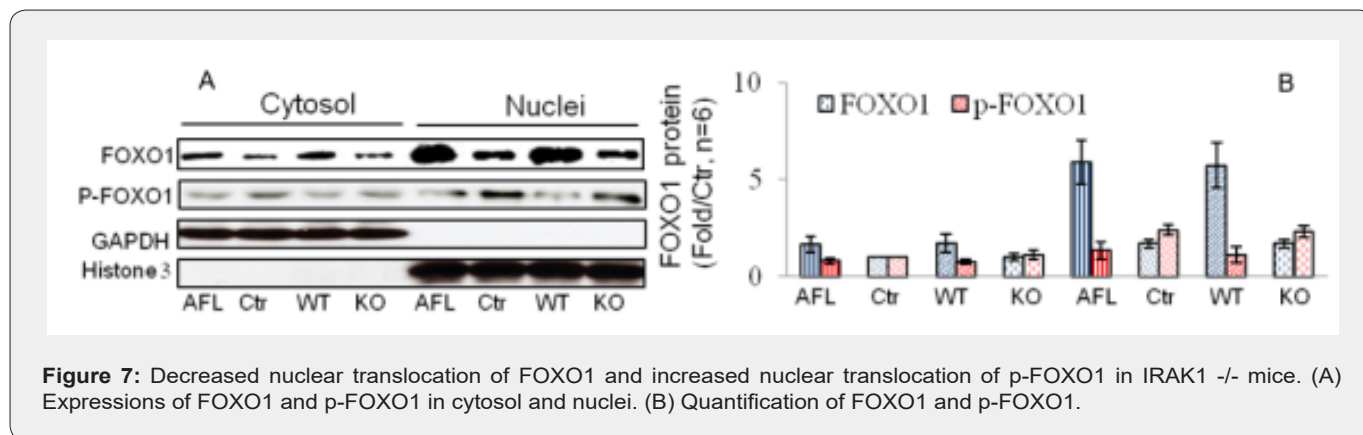


Figure 7: Decreased nuclear translocation of FOXO1 and increased nuclear translocation of p-FOXO1 in IRAK1 ^{-/-} mice. (A) Expressions of FOXO1 and p-FOXO1 in cytosol and nuclei. (B) Quantification of FOXO1 and p-FOXO1.

Discussion

Using a 7.0 T MR scanner we demonstrated that ¹H-MRS was capable of discriminating the degree of hepatic steatosis in the liver between AFL and its controls. This method was further used to discriminate decreased absolute amount in liver lipids in IRAK1^{-/-} KO mice compared with wild type mice both fed with alcohol feeding. Absolute amounts of total hepatic lipids quantified by liver ¹H MRS were strongly correlated with hepatic TG or cholesterol measured by biochemical assays either between AFL and control mice or between IRAK1^{-/-} and wild type mice. These experiments ascertain our absolute quantification method of liver lipids calculated from liver ¹H MRS – semi quantitative data is useful to represent accurate hepatic lipids in the setting of AFLD. Ethanol diet significantly up-regulates the phosphorylation of TLR4, IRAK1, STAT1, PPAR γ , and CD36 in ALF and WT mice, while down-regulating p-FOXO1 expression. However, these changes were reversed in IRAK1 ^{-/-} mice, suggested that IRAK1 gene KO can inhibit AFLD through TLR4-IRAK1-PPAR γ -CD36 pathway. Decreased expression of TLR4, but TLR2 in our IRAK1 ^{-/-} mice was found which is consistent with the study by Hritz & colleagues [20].

They investigated the alcohol-induced liver injury in wild-type, TLR2-deficient and TLR4-deficient mice, respectively after administration of the Lieber-De-Carli diet for 5 weeks. The increasing expression resulted from alcoholic feeding in wild type and TLR2 knock-out, but not in TLR4 knock-out mice. It suggested that TLR4, but not TLR2 deficiency was protective in liver injury in AFLD. More reliable evidence has demonstrated that TLR-IRAK1 signaling pathway genes were upregulated in the liver of animal models fed ethanol [21]. Our study suggests IRAK1 gene knockdown dramatically reverses hepatic pathological change and specifically, IRAK1 KO diminishes hepatic lipid accumulation caused by alcohol consumption, indicating IRAK1 gene activation may play an important role in the formation of

AFL. A study by Jiang and colleagues in male C57BL/6J mice *in vivo* and *in vitro* demonstrated that activation of TLR4 initiated that transmembrane signal cascade and triggers intracellular signal molecules including IRAK1 [22] in liver injury.

Several studies have demonstrated that STAT1 interacts with PPAR in the induction of CD36 expression. A study by Kotla & colleagues [23] has shown that STAT1 and PPAR γ complex binds to the STAT-binding site at -107 nucleotides in the CD36 promoter and enhances its activity and the interaction of STAT1 and PPAR γ depended on STAT1 acetylation. Yoo & colleagues [24] have shown that the deletion of PPAR α aggregated lipopolysaccharide (LPS)-mediated liver injury through activating STAT1 and they indicated that PPAR γ was important in preventing LPS-induced acute liver damage by regulating STAT1 signaling pathways. CD36 (also known as fatty acid translocase) is a heavily glycosylated 80 kD integral membrane protein that is widely expressed which is a class B scavenger receptor that can recognize multiple ligands, including long-chain fatty acids, oxidized lipids, and lipoproteins [25,26]. Several studies have shown that CD36 is associated with human and murine fatty liver disease and one of the possible mechanisms was via STAT1 acetylation and its interaction with PPAR.

A study by Wilson and colleagues has demonstrated that CD36 directly contributes to the development of fatty liver under conditions of elevated free fatty acids (FAs) by modulating the rate of FA uptake by hepatocytes [27]. Clugston & colleagues [13] observed increased hepatic CD36 expression in alcohol-fed mice at the gene and protein levels, they concluded that CD36 ^{-/-} mice were resistant to the lipogenic effects of consuming alcoholic liquid diet and that CD36 deficiency could protect against the development of alcoholic steatosis in mice. A study by Kotla and colleagues has shown that cholesterol crystals (CC) induced CD36 expression via STAT1 acetylation and its interaction with PPAR in mice model.

They thought that PPAR γ might be involved in the regulation of CD36 promoter activity and its expression in terms of PPAR γ antagonist inhibits the PPAR γ binding to the CD36 promoter and attenuates the promoter activity partially [28]. Our study demonstrates that CD36 may play vital role in AFLD by up-regulating the expression level of STAT1, PPAR γ , and down-regulating the expression of PPAR α . As a member of the FOXO family, FOXO1 is usually expressed in insulin-responsive tissues such as liver, adipose tissue, pancreas, etc., and participates in energy metabolism [29].

Several studies have shown that the over-expression of FOXO1 increased the synthesis of liver TG [30,31]. A study by Ren and colleagues has shown that lysophosphatidic acid/ protein kinase D1 (PKD-1) signaling leads to nuclear accumulation of histone deacetylase 7, where it interacts with FOXO1 to suppress endothelial CD36 transcription in mice model [32]. Our study suggested that alcohol-diet led to over-expression of FOXO1 both in nuclei and cytosol in terms of decreased phosphorylation of FOXO1 and resulted in the localization of nuclear and cytoplasm increased.

Then, DNA binding capacity and transcriptional activity were weakened which led to a series of downstream fat metabolism disorders.

Conclusion

IRAK1 KO has a great protective effect on ethanol-induced hepatic injury. Our study clarified that IRAK $^{-/-}$ markedly suppressed ethanol-induced hepatic steatosis, inflammation, and ballooning and concomitantly activated the signaling pathway of IRAK1 and FOXO1 and up-regulated the expression of STAT1, PPAR γ , and CD36. Therefore, IRAK1 KO can improve alcoholic hepatic steatosis by regulating IRAK1 and FOXO1 pathway and expression levels of TLR4, STAT1, PPAR γ , and CD36, thereby protecting the AFLD, and CD36 plays vital role in the pathway. Of course, longitudinal studies with a larger sample size, other animal models, different type of cells should be validated in future studies.

Acknowledgement

This work was supported by research grants from the National Institute on Alcohol Abuse and Alcoholism of the National Institutes of Health (Award Number K08AA024895-Qi Cao), R01AA028995-01-Liya Pi/sub-PI-Qi Cao), GE Healthcare & Radiological Society of North America (RSNA) Research Resident Grant (Award Number RR1250-Qi-Cao), University of Maryland Baltimore Innovative Research Grant, the Chair Research Foundation of the University of Maryland School of Medicine Department of Diagnostic Radiology and Nuclear Medicine (Qi Cao) and the Institute for Clinical & Translational Research (ICTR), the University of Maryland Baltimore (Qi Cao).

References

1. You M, Joqasuria A, Lee K, Wu J, Zhang Y, et al. (2017) Signal Transduction Mechanisms of Alcoholic Fatty Liver Disease: Emerging Role of Lipin-1. *Cur Mol Pahrmacol* 10(3): 226-236.
2. Roh YS, Seki E (2013) Toll-like receptors in alcoholic liver disease, nonalcoholic steatohepatitis and carcinogenesis. *J Gastroenterol Hepatol*, 1(0.1): 38-42.
3. Inokuchi S, Tsukamoto H, Park E, Liu ZX, Brenner DA, et al. (2011) Toll-like receptor 4 mediates alcoholic-induced steatohepatitis through bone marrow-derived and endogenous liver cells in mice. *Alcohol Clin Exp Res* 35(8): 1509-1518.
4. Gustot T, Lemmers A, Moreno C, Nagy N, Quertinmont E, et al. (2006) Differential liver sensitization to toll-like receptor pathways in mice with alcoholic fatty liver. *Hepatology* 43(5): 989-1000.
5. Markwick LJ, Riva A, Ryan JM, Cooksley H, Palma E, et al. (2015) Blockade of PD1 and TIM3 restores innate and adaptive immunity in patients with acute alcoholic hepatitis. *Gastroenterology* 148(3): 590-602.
6. Jiang W, Liu J, Dai Y, Zhou N, Ji C (2015) MiR-146b attenuates high-fat diet-induced nonalcoholic steatohepatitis in mice. *J Gastroenterol Hepatol* 30(5): 933-943.
7. Wang L, Qiao Q, Ferrao R, Shen C, Hatcher JM, et al. (2017) Crystal structure of human IRAK1. *Proc Natl Acad Sci USA* 114(51): 13507-13512.
8. Tomita K, Kabashima A, Freeman BL, Bronk SF, Hirsova P (2017) Mixed lineage Kinase 3 Mediates the Induction of CXCL10 by a STAT1-Dependant Mechanism During Hepatocyte Lipotoxicity. *J Cell Biochem* 118(10): 3249-3259.
9. Zhang Y, Gan Z, Huang P, Zhou L, Mao T, et al. (2012) A role of protein inhibitor of activated STAT1 (PIAS1) in lipogenic regulation through SUMOylation-independent suppression of liver X receptor. *J Bio Chem* 287(45): 37973-37985.
10. Kim MJ, Sim MO, Lee HI, Ham JR, Seo KI, et al. (2014) Dietary umbelliferone attenuates alcohol-induced fatty liver via regulation of PPAR α and SREBP1c in rats. *Alcohol* 48(7): 707-715.
11. Zhang W, Sun Q, Zhang W, Sun X, Zhou Z (2016) Hepatic Peroxisome Proliferator-Activated Receptor Gamma Signaling Contributes to Alcohol-induced Hepatic Steatosis and Inflammation in Mice. *Alcohol Clin Exp Res* 40(5): 988-999.
12. Xu MJ, Cai Y, Wang H, Altamirano J, Chang B, et al. (2015) Fat-Specific Protein 27/CIDEA Promotes Development of Alcoholic Steatohepatitis in Mice and Humans. *Gastroenterology* 149(4): 1030-1041.
13. Clugston RD, Yuen JJ, Hu Y, Abumrad NA, Berk PD, et al. (2014) CD36-deficient mice are resistant to alcohol- and high-carbohydrate-induced hepatic steatosis. *J Lipid Res* 55(2): 239-246.
14. Handberg A, Højlund K, Gastaldelli A, Flyvbjerg A, Dekker JM, et al. (2012) Plasma sCD36 is associated with markers of atherosclerosis, insulin resistance and fatty liver in a nondiabetic healthy population. *J Intern Med* 271(3): 294-304.
15. Shirpoor A, Heshmati E, Kheradmand F, Gharalari FH, Chodari L, et al. (2018) Increased hepatic FAT/CD36, PTP1B and decreased HNF4A expression contributes to dyslipidemia associated with ethanol-induced liver dysfunction: Rescue effect of ginger extract. *Biomed Pharmacother* 105: 144-150.
16. Sun Z, Zhou JY (2016) Mechanism of action of the SIRT1-FoxO1-Adipo R2 signaling pathway in alcoholic fatty liver disease. *Zhonghua Gan Zang Za Zhi* 24(11): 877-880.

17. Zhu W, Chen S, Li Z, Zhao X, Li W, et al. (2014) Effects and mechanisms of resveratrol on the amelioration of oxidative stress and hepatic steatosis in KKAY mice. *Nutr Metab (Lond)* 11: 35.
18. Xu S, Zhu W, Wan Y, Chen X, Pi L, et al. (2018) Decreased Taurine and Creatine in the Talamus May Related to Behavioral Impairments in Ethanol-Fed Mice: A Pilot Study of Proton Magnetic Resonance Spectroscopy. *Mol Imaging* 17.
19. Cao Q, Batey R, Pang G, Clancy R (1999) Ethanol-altered liver-associated T cells mediate liver injury in rats administered Concanavalin A (Con A) or lipopolysaccharide (LPS). *Alcohol Clin Exp Res* 23(10): 1660-1667.
20. Hritz I, Mandrekar P, Velayudham A, Catalano D, Dolganiuc A, et al. (2008) The critical role of toll-like receptor (TLR) 4 in alcoholic liver disease is independent of the common TLR adaptor MyD88. *Hepatology*, 48(4): 1224-1231.
21. Khachatoorian R, Dawson D, Maloney EM, Wang J, French BA, et al. (2013) SAME treatment prevents the ethanol-induced epigenetic alterations of genes in the Toll-like receptor pathway. *Exp Mol Pathol* 94(1): 243-246.
22. Jiang W, Kong L, Ni Q, Lu Y, Ding W, et al. (2014) miR-146 ameliorates liver ischemia/reperfusion injury by suppressing IRAK1 and TRAF6. *Plos One* 9(7).
23. Kotla S, Rao GN (2015) Reactive Oxygen Species (ROS) Mediate p300-dependent STAT1 Protein Interaction with Peroxisome Proliferator-activated Receptor (PPAR)- γ in CD36 Protein Expression and Foam Cell Formation. *J Biol Chem* 290(5): 30306-30320.
24. Yoo SH, Park O, Henderson LE, Abdelmegeed MA, Moon KH, et al. (2011) Lack of PPAR α exacerbates lipopolysaccharide-induced liver toxicity through STAT1 inflammatory signaling and increased oxidative/nitrosative stress. *Toxicol Lett* 202(1): 23-29.
25. Pepino MY, Kuda O, Samovski D, Abumrad NA (2014) Structure-function of CD36 and importance of fatty acid signal transduction in fat metabolism. *Annu Rev Nutr* 34: 281-303.
26. Silverstein RL, Febbraio M (2009) CD36, a scavenger receptor involved in immunity, metabolism, angiogenesis, and behavior. *Sci Signal* 2(72).
27. Wilson CG, Tran JL, Erion DM, Vera NB, Febbraio M (2016) Hepatocyte-Specific Disruption of CD36 Attenuates Fatty Liver and Improves Insulin Sensitivity in HFS-Fed Mice. *Endocrinology* 157(2): 570-585.
28. Kotla S, Singh NK, Rao GN (2017) ROS via BTK-P300-STAT1-PPAR γ signaling activation mediates cholesterol crystals-induced CD36 expression and foam cell formation. *Redox Biol* 11: 350-364.
29. Dowell P, Otto TC, Adi S, Lane MD (2003) Convergence of peroxisome proliferator-activated receptor gamma and Foxo1 signaling pathways. *J Biol Chem* 278(46): 45485-45491.
30. Cheng Q, Li YW, Yang CF, Zhong YJ, He H, et al. (2018) Methyl ferulic acid attenuates ethanol-induced hepatic steatosis by regulating AMPK and Fox1 Pathways in Rats and L-02 cells. *Chem Biol Interact* 291: 180-189.
31. Li Y, Wu S (2018) Epigallocatechi gallate suppressed hepatic cholesterol synthesis by targeting SREBP-2 through SIRT1/FOXO1 signaling pathway. *Mol Cell Biochem* 448(1-2): 175-185.
32. Ren B, Best B, Ramakrishnan DP, Walcott BP, Storz P, et al. (2016) LPA/PKD-1-FoxO1 Signaling Axis Mediates Endothelial Cell CD36 Transcriptional Repression and Proangiogenic and Proarteriogenic Reprogramming. *Arterioscler Thromb Vasc Biol* 36(6): 1197-1208.



This work is licensed under Creative Commons Attribution 4.0 License
DOI: [10.19080/ARGH.2021.18.555983](https://doi.org/10.19080/ARGH.2021.18.555983)

**Your next submission with JuniperPublishers
will reach you the below assets**

- Quality Editorial service
- Swift Peer Review
- Reprints availability
- E-prints Service
- Manuscript Podcast for convenient understanding
- Global attainment for your research
- Manuscript accessibility in different formats
(Pdf, E-pub, Full Text, audio)
- Unceasing customer service

Track the below URL for one-step submission
<https://juniperpublishers.com/online-submission.php>